*Inorg. Chem.* **2002**, *41*, 3280–3290


# A Mechanistic Investigation of Oxidative Addition of Methyl Iodide to [Tp*Rh(CO)(L)]

**Valérie Chauby,[†] Jean-Claude Daran,[‡] Carole Serra-Le Berre,[†] François Malbosc,[†] Philippe Kalck,*[,†] Oscar Delgado Gonzalez,[§] Claire E. Haslam,[§] and Anthony Haynes*[,§]**

*Laboratoire de Catalyse Chimie Fine et Polymères, Ecole Nationale Superieure des Ingénieurs en Arts Chimiques et Technologiques, 118 route de Narbonne, 31077 Toulouse Cedex 4, France, Laboratoire de Chimie de Coordination du CNRS, associée à l'Université Paul Sabatier et à l'Institut Polytechnique de Toulouse, 205 route de Narbonne, 31078 Toulouse Cedex 4, France, and Department of Chemistry, University of Sheffield, Sheffield, U.K., S3 7HF*

Received March 14, 2002

Reaction of methyl iodide with square planar [$\kappa^2$-Tp*Rh(CO)($PMe_3$)] **1a** (Tp* = HB(3,5-$Me_2$pz)$_3$) at room temperature affords [$\kappa^3$-Tp*Rh(CO)($PMe_3$)(Me)]I **2a**, which was fully characterized by spectroscopy and X-ray crystallography. The pseudooctahedral geometry of cationic **2a**, which contains a $\kappa^3$-coordinated Tp* ligand, indicates a reaction mechanism in which nucleophilic attack by Rh on MeI is accompanied by coordination of the pendant pyrazolyl group. In solution **2a** transforms slowly into a neutral (acetyl)(iodo) rhodium complex [$\kappa^3$-Tp*Rh($PMe_3$)(COMe)I] **3a**, for which an X-ray crystal structure is also reported. Kinetic studies on the reactions of [$\kappa^2$-Tp*Rh(CO)(L)] (L = $PMe_3$, $PMe_2Ph$, $PMePh_2$, $PPh_3$, CO)] with MeI show second-order behavior with large negative activation entropies, consistent with an $S_N2$ mechanism. The second-order rate constants correlate well with phosphine basicity. For L = CO, reaction with MeI gives an acetyl complex, [$\kappa^3$-Tp*Rh(CO)(COMe)I]. The bis(pyrazolyl)borate complexes [$\kappa^2$-Bp*Rh(CO)(L)] (L = $PPh_3$, CO) are much less reactive toward MeI than the Tp* analogues, indicating the importance of the third pyrazolyl group and the accessibility of a $\kappa^3$ coordination mode. The results strengthen the evidence in favor of an $S_N2$ mechanism for oxidative addition of MeI to square planar $d^8$ transition metal complexes.

## Introduction

The oxidative addition reaction occupies a central position in the activation of small molecules by electron-rich transition metal complexes and in homogeneous catalysis. A classic example is the addition of alkyl halides to square planar $d^8$ metal complexes,[1] the reaction of $[M(CO)_2I_2]^-$ (M = Rh or Ir) with methyl iodide being a key step in the homogeneous catalytic carbonylation of methanol.[2] It is widely accepted that oxidative addition of MeI occurs via a two-step mechanism (Scheme 1) involving (i) nucleophilic attack by the metal on the methyl carbon to displace iodide and form a metal−carbon bond and (ii) coordination of iodide to the five-coordinate intermediate. Depending upon the stereochemical rigidity of the intermediate complex, the methyl and iodide ligands can be placed mutually trans or cis in the octahedral product (although observation of cis products has sometimes been taken as evidence for an alternative concerted three-centered mechanism[3]). For higher alkyl halides, radical mechanisms are also thought to participate.[4]

**Scheme 1.** $S_N2$ Mechanism for Oxidative Addition of MeI to a Square Planar Complex

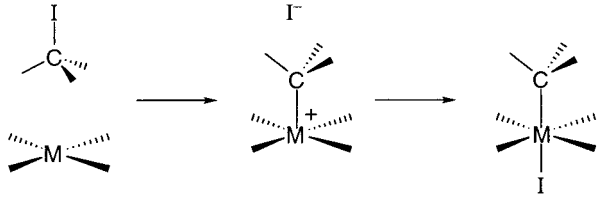


* Authors to whom correspondence should be addressed. E-mail: a.haynes@sheffield.ac.uk (A.H.); pkalck@ensct.fr (P.K.).
[†] Ecole Nationale Superieure des Ingénieurs en Arts Chimiques et Technologiques.
[‡] Laboratoire de Chimie de Coordination du CNRS, associée à l'Université Paul Sabatier et à l'Institut Polytechnique de Toulouse.
[§] University of Sheffield.

(1) Stille, J. K.; Lau, K. S. Y. *Acc. Chem. Res.* **1977**, *10*, 434. Henderson, S.; Henderson, R. A. *Adv. Phys. Org. Chem.* **1987**, *23*, 1.
(2) Maitlis, P. M.; Haynes, A.; Sunley, G. J.; Howard, M. J. *J. Chem. Soc., Dalton Trans.* **1996**, 2187.



10.1021/ic0255959 CCC: $22.00 
Published on Web 05/18/2002

The two-step $S_N2$ mechanism is supported by the observation of second-order kinetics with large negative activation entropies indicating a highly ordered transition state.[5] Recent theoretical studies have also favored an $S_N2$ mechanism.[6] For neutral reactant complexes, polar solvents promote the reaction rate due to their ability to solvate and therefore stabilize the intermediate ion pair.[5] In the case of certain Pt(II) complexes, $[L_2Pt(Me)_2]$, direct NMR spectroscopic evidence was obtained for the solvated cationic intermediate, $[L_2Pt(Me)_2(R)(NCMe)]^+$, during oxidative addition of alkyl halides.[7] In this paper we report how the cationic intermediate resulting from the $S_N2$ step can be stabilized by *intramolecular* trapping, using the pendant pyrazolyl group of a $\kappa^2$-coordinated tris(pyrazolyl)borate ligand.

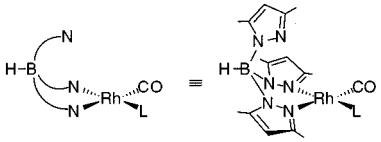

| Complex | L |
|---|---|
| **1a** | $PMe_3$ |
| **1b** | $PMe_2Ph$ |
| **1c** | $PMePh_2$ |
| **1d** | $PPh_3$ |

Some of us have recently reported the synthesis of a series of complexes [Tp*Rh(CO)(L)] **1** (Tp* = $HB(3,5\text{-}Me_2pz)_3$) containing a range of phosphorus donor ligands L.[8,9] X-ray crystallographic and spectroscopic studies showed that the phosphine complexes **1a**−**d** all have square planar structures with $\kappa^2$ Tp* ligands, in contrast to the dicarbonyl precursor **1e** (L = CO) which is five coordinate with a $\kappa^3$ Tp* ligand. The square planar geometry of **1d** has also been reported by Connelly et al.[10,11] The relatively low $\nu$(CO) frequencies (1969−1979 $cm^{-1}$) shown by **1a**−**d** reveal a high electron density on the rhodium center, making these complexes good candidates for oxidative addition reactions. The presence of a pendant pyrazolyl group introduces the potential for intercepting coordinatively unsaturated intermediate species.


(3) Venter, J. A.; Leipoldt, J. G.; van Eldik, R. *Inorg. Chem.* **1991**, *30*, 2207. Damoense, L. J.; Purcell, W.; Roodt, A. *Rhodium Express* **1995**, *14*, 4. Galding, M. R.; Cherkasova, T. G.; Osetrova, L. V.; Varshavsky, Y. S.; Roodt, A. *Rhodium Express* **1996**, *16*, 23. Roodt, A.; Botha, J. M.; Otto, S.; Shestakova, E. P.; Varshavsky, Y. S. *Rhodium Express* **1996**, *17*, 4.

(4) Labinger, J. A.; Osborn, J. A. *Inorg. Chem.* **1980**, *19*, 3230. Labinger, J. A.; Osborn, J. A.; Coville, N. J. *Inorg. Chem.* **1980**, *19*, 3236.

(5) Chock, P. B.; Halpern, J. *J. Am. Chem. Soc.* **1966**, *88*, 3511.

(6) Griffin, T. R.; Cook, D. B.; Haynes, A.; Pearson, J. M.; Monti, D.; Morris, G. E. *J. Am. Chem. Soc.* **1996**, *118*, 3029. Kinnunen, T.; Laasonen, K. *J. Mol. Struct. (THEOCHEM)* **2001**, *542*, 273. Ivanova, E. A.; Gisdakis, P.; Nasluzov, V. A.; Rubailo, A. I.; Rösch, N. *Organometallics* **2001**, *20*, 1161.

(7) Crespo, M.; Puddephatt, R. J. *Organometallics* **1987**, *6*, 2548. Puddephatt, R. J.; Scott, J. D. *Organometallics* **1985**, *4*, 1221.

(8) Chauby, V.; Berre, C. S. L.; Kalck, P.; Daran, J.-C.; Commenges, G. *Inorg. Chem.* **1996**, *35*, 6354.

(9) Malbosc, F.; Chauby, V.; Berre, C. S.-L.; Etienne, M.; Daran, J.-C.; Kalck, P. *Eur. J. Inorg. Chem.* **2001**, 2689.

(10) Connelly, N. G.; Emslie, D. J. H.; Metz, B.; Orpen, A. G.; Quayle, M. J. *Chem. Commun.* **1996**, 2289.

(11) Connelly, N. G.; Emslie, D. J. H.; Geiger, W. E.; Hayward, O. D.; Linehan, E. B.; Orpen, A. G.; Quayle, M. J.; Rieger, P. H. *J. Chem. Soc., Dalton Trans.* **2001**, 670.


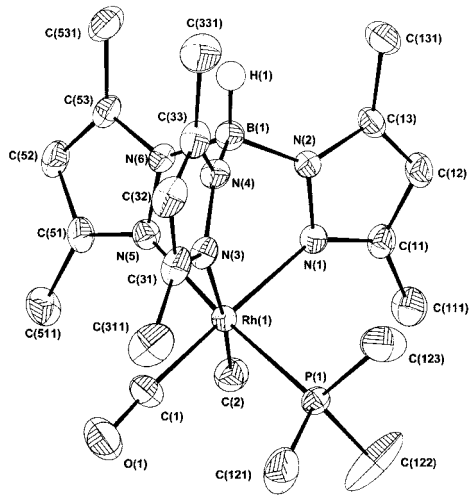


**Figure 1.** CAMERON view of **2a**. Thermal ellipsoids are shown at the 50% probability level. Hydrogen atoms and iodide counterion are omitted for clarity.

**Table 1.** Selected Bond Distances (Å) and Angles (deg) for **2a**

| | | | |
|---|---|---|---|
| Rh(1)−P(1) | 2.3166(9) | Rh(1)−N(1) | 2.138(3) |
| Rh(1)−C(1) | 1.855(4) | Rh(1)−N(3) | 2.237(3) |
| Rh(1)−C(2) | 2.090(5) | Rh(1)−N(5) | 2.119(3) |
| P(1)−Rh(1)−N(1) | 91.72(7) | N(1)−Rh(1)−C(2) | 89.3(1) |
| P(1)−Rh(1)−N(3) | 92.87(7) | N(3)−Rh(1)−N(5) | 83.5(1) |
| P(1)−Rh(1)−C(1) | 89.31(1) | N(3)−Rh(1)−C(1) | 92.8(2) |
| P(1)−Rh(1)−N(5) | 174.55(8) | N(3)−Rh(1)−C(2) | 173.81(1) |
| N(1)−Rh(1)−N(3) | 92.51(1) | N(5)−Rh(1)−C(1) | 94.9(1) |
| N(1)−Rh(1)−N(5) | 84.4(1) | N(5)−Rh(1)−C(2) | 90.9(1) |
| N(1)−Rh(1)−C(1) | 174.5(2) | C(1)−Rh(1)−C(2) | 85.3(2) |

## Results and Discussion

**Oxidative Addition of MeI to [Tp*Rh(CO)(L)].** The reaction of [Tp*Rh(CO)($PMe_3$)] **1a** with a stoichiometric amount of methyl iodide in toluene at 20 °C resulted in formation of a white precipitate, which was isolated by filtration and recrystallized from dichloromethane/heptane. The IR spectrum of the product **2a** displayed a single intense $\nu$(CO) absorption at 2080 $cm^{-1}$, consistent with a Rh(III) species retaining a terminal CO ligand. NMR spectroscopy revealed $^1H$ and $^{13}C$ resonances of a methyl ligand with coupling to both $^{103}Rh$ and $^{31}P$, together with six distinct methyl resonances due to the three inequivalent $Me_2pz$ groups of the Tp* ligand. Spectroscopic characterization of the product as [Tp*Rh(CO)($PMe_3$)Me]I **2a** was confirmed by an X-ray crystal structure, shown in Figure 1, which reveals a cationic rhodium methyl complex for which iodide is the counterion. The Tp* ligand adopts $\kappa^3$ coordination to complete a pseudooctahedral environment about the Rh center, in contrast to the $\kappa^2$ Tp* ligand in the square planar precursor **1a**. Selected bond distances and angles for **2a** are given in Table 1. The Rh−$CH_3$, Rh−CO, and Rh−P bond lengths are comparable to those found in other cationic complexes, e.g., [CpRh(CO){(*S*)-($PPh_2NHCHMePh$)}Me]$^+$ [12] and [(2,4-$Me_2Cp$)Rh($PEt_3$)$_2$Me]$^+$.[13] For the Tp* ligand, the Rh−N(3) distance (2.237(3) Å) is significantly longer than the Rh−N(1) and Rh−N(5) distances (respectively 2.138(3)


(12) Quinn, S.; Shaver, A. *J. Am. Chem. Soc.* **1982**, *104*, 1096.

(13) Bleeke, J. R.; Donaldson, A. J. *Organometallics* **1988**, *7*, 1588.

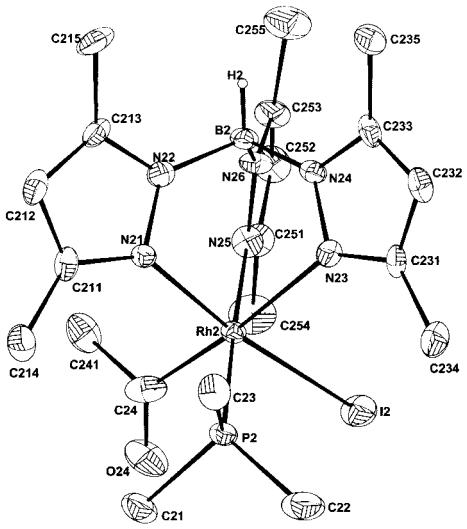


**Figure 2.** CAMERON view of **3a**. Thermal ellipsoids are shown at the 50% probability level. Hydrogen atoms are omitted for clarity.

**Scheme 2.** Reactions of **1a**−**c** with MeI

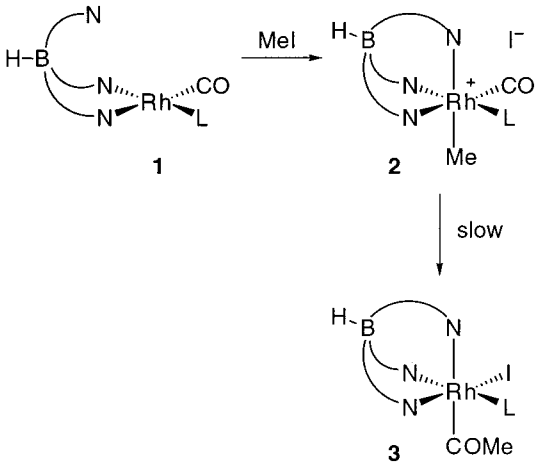


and 2.119(3) Å) in accordance with the greater trans influence of methyl relative to phosphine and carbonyl ligands.

In dichloromethane, under ambient conditions, **2a** was transformed slowly into another species, **3a**, which displayed an IR absorption at 1670 $cm^{-1}$ consistent with the presence of an acetyl ligand. $^1H$ NMR spectroscopy showed a singlet at 2.09 for the acetyl group and six signals for the $Me_2pz$ methyl groups. As monitored by NMR, 40% conversion of **2a** into **3a** had occurred after 1 day and conversion was complete after several days. Slow evaporation of $CD_2Cl_2$ at room temperature afforded orange crystals, which were analyzed by X-ray crystallography. The structure displayed in Figure 2 shows an (iodo)(acetyl) complex [Tp*Rh($PMe_3$)(COMe)I] **3a** resulting from migratory CO insertion in the cation **2a** and coordination of the iodide counterion to give a neutral product (Scheme 2). The asymmetric unit contains two distinct molecules of **3a** with very similar geometries, each present as a pair of enantiomers in the unit cell. Geometric data for one of the molecules are given in Table 2. The rhodium center is in a pseudooctahedral environment with Rh−I, Rh−P, and Rh−C(O)$CH_3$ bond distances comparable with those reported for [CpRh{(*S*)-($PPh_2$-NHCHMePh)}(COMe)I].[12] The Rh−N bond trans to acetyl (2.402(6) and 2.378(6) Å in the two molecules) is significantly longer than the Rh−N bonds trans to phosphine (2.138(6) and 2.140(6) Å) or iodide (2.100(6) and 2.125(6) Å) in accordance with the high trans influence of acetyl. Comparison of the Rh−N bond lengths in **2a** and **3a** also indicates that acetyl has a stronger trans influence than methyl.

**Table 2.** Selected Bond Distances (Å) and Angles (deg) for Molecule 1 of **3a**

| | | | |
|---|---|---|---|
| Rh(1)−P(1) | 2.301(2) | Rh(1)−N(1) | 2.101(6) |
| Rh(1)−I(1) | 2.6294(7) | Rh(1)−N(3) | 2.402(6) |
| P(1)−C(1) | 1.795(1) | Rh(1)−N(5) | 2.138(6) |
| Rh(1)−C(4) | 2.042(8) | | |
| I(1)−Rh(1)−P(1) | 89.29(6) | P(1)−Rh(1)−C(4) | 93.4(3) |
| I(1)−Rh(1)−N(1) | 176.72(16) | N(3)−Rh(1)−C(4) | 174.7(3) |
| I(1)−Rh(1)−N(3) | 89.63(17) | N(5)−Rh(1)−N(3) | 88.6(2) |
| I(1)−Rh(1)−N(5) | 90.06 (16) | N(1)−Rh(1)−N(1) | 87.3(3) |
| I(1)−Rh(1)−C(4) | 91.2(2) | N(1)−Rh(1)−C(4) | 90.9(3) |
| P(1)−Rh(1)−N(1) | 93.13(19) | N(3)−Rh(1)−N(5) | 84.3(2) |
| P(1)−Rh(1)−N(3) | 91.82(19) | N(3)−Rh(1)−C(4) | 174.7(3) |
| P(1)−Rh(1)−N(5) | 176.10(17) | N(5)−Rh(1)−C(4) | 90.4(5) |

The reaction of [Tp*Rh(CO)($PMe_2Ph$)] **1b** with MeI was also found to give a Rh(III) methyl product, [Tp*Rh(CO)($PMe_2Ph$)Me]I **2b**, which was isolated and characterized. IR spectroscopy revealed that slow conversion of **2b** into the acetyl complex **3b** ($\nu$(CO) 1658 $cm^{-1}$) occurred in $CH_2Cl_2$ solution. The reactions of **1c** and **1d** with MeI exhibited similar behavior when monitored by IR spectroscopy, giving absorptions at 2085 and 2082 $cm^{-1}$ respectively for methyl complexes **2c** and **2d** and at 1659 and 1692 $cm^{-1}$ respectively for acetyl complexes **3c** and **3d**. The products of these reactions were not isolated.

In addition to the phosphine complexes **1a**−**d** we also studied the reaction of methyl iodide with the dicarbonyl complex **1e**. In contrast to the square planar phosphine complexes, the dominant form of **1e** is a five-coordinate $\kappa^3$ complex ($\nu$(CO) 2057, 1981 $cm^{-1}$ in $CH_2Cl_2$) in equilibrium with a small amount of the $\kappa^2$ isomer ($\nu$(CO) 2080, 2012 $cm^{-1}$).[14] After a solution of **1e** in $CH_2Cl_2$ containing a large excess of methyl iodide was stirred, the IR spectrum showed bands at 2068 and 1682 $cm^{-1}$, indicating a product with both terminal and acetyl CO ligands. On reduction of the solvent and cooling to 0 °C, a dark red precipitate was formed. The $^1H$ NMR spectrum showed three singlets due to H-4 of three inequivalent pyrazolyl groups, along with a singlet due to an acetyl ligand at $\delta$ 2.65, although a number of signals due to impurities were also present. The spectroscopic data are consistent with a major product of formula [Tp*Rh(CO)(COMe)I] **3e**, presumably resulting from rapid migratory CO insertion in an unobserved (methyl)(carbonyl) intermediate (Scheme 3). The reaction is analogous to the addition of MeI to [Cp*Rh($CO)_2$], which gives [Cp*Rh(CO)(COMe)I].[15] Methyl migration is clearly much more facile in the dicarbonyl system than in the phosphine complexes **2a**−**d**, as

(14) Ball, R. G.; Ghosh, C. K.; Hoyano, J. K.; McMaster, A. D.; Graham, W. A. G. *J. Chem. Soc., Chem. Commun.* **1989**, 341.
(15) Kang, J. W.; Maitlis, P. M. *J. Organomet. Chem.* **1971**, *26*, 393.

**Scheme 3.** Reaction of **1e** with MeI

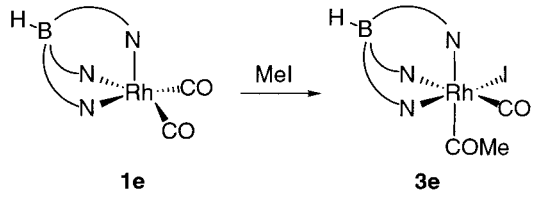


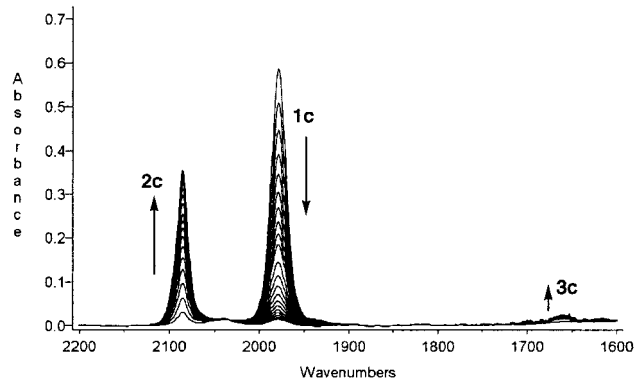


**Figure 3.** A series of IR spectra during the reaction of **1c** with MeI (0.8 M) in $CH_2Cl_2$ at 25 °C.

found in related systems where coordination of electron-donating phosphines tends to retard migratory CO insertion.[16−18]

**Kinetic Measurements for Addition of MeI to 1a−e.** Kinetic measurements for the reactions of the complexes **1a**−**e** with methyl iodide in $CH_2Cl_2$ were carried out using IR spectroscopy to monitor changes in the $\nu$(CO) bands due to reactants and products. Pseudo-first-order conditions (at least 10-fold excess MeI) were employed. A typical series of spectra for the reaction of **1c** is shown in Figure 3 showing the disappearance of the $\nu$(CO) band of the reactant complex at 1979 $cm^{-1}$ and the appearance of a new absorption at 2085 $cm^{-1}$ assigned to the Rh(III) methyl product, [Tp*Rh(CO)-($PMePh_2$)Me]I **2c**. A very weak absorption is also apparent at 1659 $cm^{-1}$ due to formation of a small amount of the acetyl product [Tp*Rh($PMePh_2$)(COMe)I] **3c** resulting from slow migratory insertion in **2c**.[19] For the reactions of **1a**−**c**, the exponential decay observed for the reactant $\nu$(CO) band showed the reactions to be first order in [complex]; observed pseudo-first-order rate constants ($k_{obs}$) are given in the Supporting Information. Plots of $k_{obs}$ vs [MeI] are linear (Figure 4), indicating the reactions to be first order in MeI and hence second order overall. Second-order rate constants ($k_2$) are given in Table 3. Variable-temperature kinetic data over the range 5−35 °C were also measured, and satisfactory

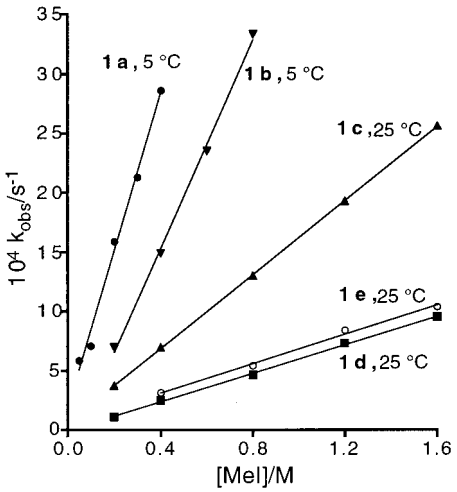


**Figure 4.** Plots showing linear dependence of $k_{obs}$ on [MeI] for the reactions of **1a**−**e** with MeI in $CH_2Cl_2$.

**Table 3.** Second Order Rate Constants $k_2$ (25 °C) and Activation Parameters (with Standard Deviations) for the Reactions of **1a**−**e** with MeI in $CH_2Cl_2$

| complex | L | $\nu$(CO)/ $cm^{-1}$ | $10^4k_2$/ $M^{-1}\,s^{-1}$ | $\Delta H^{\ddagger}$/ kJ $mol^{-1}$ | $\Delta S^{\ddagger}$/ J $mol^{-1}\,K^{-1}$ |
|---|---|---|---|---|---|
| **1a** | $PMe_3$ | 1969 | 248 | 39 (±1) | −144 (±3) |
| **1b** | $PMe_2Ph$ | 1973 | 137 | 44 (±2) | −132 (±5) |
| **1c** | $PMePh_2$ | 1979 | 15.6 | 39 (±2) | −167 (±6) |
| **1d**[a] | $PPh_3$ | 1978 | 5.51 | 50 (±1) | −142 (±6) |
| **1e**[a] | CO | 2057, 1981 | 6.21 | 48 (±2) | −145 (±8) |

[a] Measured in the presence of Proton Sponge (10-fold excess/Rh).

linear Eyring plots of these data gave the activation parameters listed in Table 3.

The reaction of the $PPh_3$ complex **1d** with methyl iodide was somewhat more complicated. Decay of the $\nu$(CO) band of **1d** at 1978 $cm^{-1}$ was accompanied by growth of a new peak at 2082 $cm^{-1}$, assigned to [Tp*Rh(CO)(Me)($PPh_3$)]I **2d**, by analogy with the corresponding methyl complexes **2a**−**c**. This band also displays a shoulder at 2094 $cm^{-1}$. As the reaction proceeded, the 2082 $cm^{-1}$ peak reached a maximum and then slowly decayed, accompanied by the growth of a further band at 2068 $cm^{-1}$. An absorption also appeared slowly at 1692 $cm^{-1}$, consistent with formation of the acetyl product **3d**. A further complication was that the1978 $cm^{-1}$ band of **1d** appeared to shift to higher frequency as the reaction progressed, eventually giving a band at 1988 $cm^{-1}$. An explanation for this behavior was found by examining the reactivity of **1d** toward a strong acid. Treatment of **1d** with a stoichiometric amount of $HBF_4{\cdot}OEt_2$ in $CH_2Cl_2$ rapidly gave a product with a $\nu$(CO) band at 1988 $cm^{-1}$, corresponding to the "shifted" band observed in the kinetics experiment. Recrystallization from $CH_2Cl_2-Et_2O$ gave an orange solid, which was characterized by NMR spectroscopy and elemental analysis as [{$\kappa^2$-HB(3,5-$Me_2$pz)$_2$-(3,5-$Me_2$pzH)}Rh(CO)($PPh_3$)]$BF_4$ **4d**. This product results from N-protonation of the pendant pyrazolyl group of the Tp* ligand in **1d**, as shown by the singlet due to N−H at 12.05 in the $^1$H NMR spectrum. The relatively small (10 $cm^{-1}$) shift of $\nu$(CO) to higher frequency also supports protonation at nitrogen rather than Rh. Analogous N-proto-

(16) Rankin, J.; Benyei, A. C.; Poole, A. D.; Cole-Hamilton, D. J. *J. Chem. Soc., Dalton Trans.* **1999**, 3771.
(17) Gonsalvi, L.; Adams, H.; Sunley, G. J.; Ditzel, E.; Haynes, A. *J. Am. Chem. Soc.* **1999**, *121*, 11233.
(18) Cavallo, L.; Sola, M. *J. Am. Chem. Soc.* **2001**, *123*, 12294.
(19) For kinetic experiments using **1a**, in addition to the band due to **2a** at 2082 $cm^{-1}$ a weaker IR band was observed to grow at 2052 $cm^{-1}$. Although no further characterization of this species was attempted, the frequency is consistent with a neutral Rh(III) carbonyl complex, [$\kappa^2$-Tp*Rh(CO)($PMe_3$)(Me)I], resulting from MeI oxidative addition to **1a** with the Tp* ligand remaining bidentate. This species was not formed in the preparative reaction in toluene.

**Scheme 4.** Reactions of **1d** with MeI and $H^+$

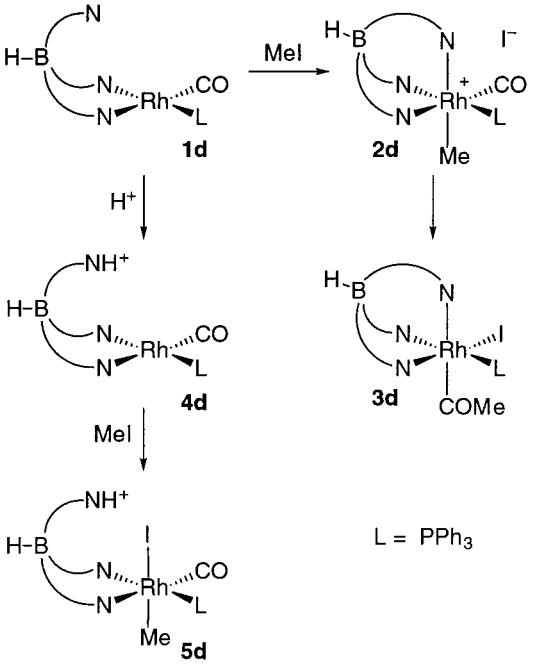


**Scheme 5.** Reactions of **1e** with MeI and $H^+$

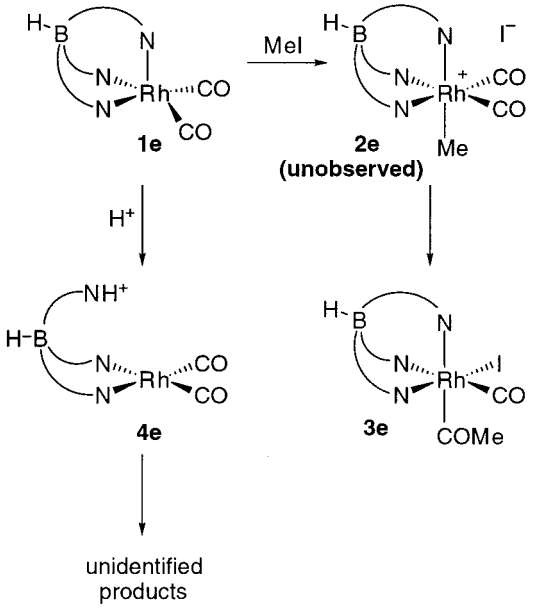


nation occurs for **1b**[9] and the dicarbonyl **1e**.[14,20] Treatment of the cationic complex **4d** with excess methyl iodide resulted in the very slow formation (over a period of 1 week) of an IR band at 2094 $cm^{-1}$, corresponding to the position of a weak shoulder observed in the kinetic experiments. We tentatively assign this feature to [{$\kappa^2$-HB(3,5-$Me_2$pz)$_2$(3,5-$Me_2$pzH)}Rh(CO)(Me)($PPh_3$)I]$BF_4$ **5d**, resulting from oxidative addition of MeI to **4d**. The reactivity observed for **1d** is summarized in Scheme 4.

The source of $H^+$ for N-protonation of **1d** is uncertain but likely results from the presence of trace water or HCl in the chlorinated solvent. This behavior was not observed for the analogous phosphine complexes **1a**−**c**, presumably because of their faster reactions with MeI which compete effectively with any side reaction. In order to improve the kinetic data for the $PPh_3$ system, we carried out studies of the reaction of **1d** with MeI in the presence of Proton Sponge (1,8-bis(dimethylamino)naphthalene), a strong, nonnucleophilic base (10-fold excess/Rh). Under these conditions, simplified IR spectra were obtained indicating a cleaner reaction, with the shift of $\nu$(CO) from 1978 $cm^{-1}$ (**1d**) to 1988 $cm^{-1}$ (**4d**) being almost completely suppressed, along with the unassigned band at 2068 $cm^{-1}$. Analysis of the exponential decay of the 1978 $cm^{-1}$ band of **1d** gave pseudo-first-order rate constants reported in the Supporting Information and plotted in Figure 4. First-order dependence on both [**1d**] and [MeI] was found, and the calculated second-order rate constant and activation parameters are given in Table 3.[21]

When the reaction of **1e** with MeI (1.6 M in $CH_2Cl_2$) was monitored by IR spectroscopy in a kinetic experiment, the behavior was again unexpectedly complicated. The decay of the two terminal $\nu$(CO) bands of **1e** at 2057 and 1982 $cm^{-1}$ was accompanied by the growth of absorptions due to the product acetyl complex **3e** at 2069 and 1681 $cm^{-1}$. However, two additional bands (2090 and 2025 $cm^{-1}$) also appeared with significant intensity in the terminal $\nu$(CO) region. Analysis of the time dependence of these bands shows that they reach maximum intensity after about 800 s and then slowly decay over a period of 2−3 h. The bands due to the acetyl product **3e** stop growing after about 1500 s, remaining steady until the end of the experiment. Therefore the species responsible for the 2090 and 2025 $cm^{-1}$ bands does not convert to **3e**, ruling out the possibility that these bands are due to an intermediate rhodium methyl species [Tp*Rh(CO)$_2$Me]I **2e**.[22] As for the $PPh_3$ system (vide supra), these observations can be accounted for by N-protonation of a pyrazolyl group of the Tp* ligand. The IR bands we observe at 2090 and 2025 $cm^{-1}$ correspond with those reported for [{$\kappa^2$-HB(3,5-Mepz)$_2$(3,5-MepzH)}Rh(CO)$_2$]$BF_4$ formed by reaction of **1e** with $HBF_4$·$OEt_2$.[14,20] The slow decay of this species in our experiments indicates a side reaction or decomposition pathway.[23] These observations are summarized in Scheme 5.

The N-protonation route was again suppressed by carrying out the reactions with methyl iodide in the presence of Proton Sponge (10-fold excess/Rh). Under these conditions, formation of the N-protonated species with bands at 2090 and 2025 $cm^{-1}$ was completely inhibited and kinetic measurements showed clean second-order behavior. The observed pseudo-

(20) Purwoko, A. A.; Lees, A. J. *Inorg. Chem.* **1996**, *35*, 675.
(21) In view of the difficulties encountered in making kinetic measurements for **1d** and **1e**, our confidence in the accuracy of these data is not as high as for complexes **1a**−**c**.
(22) The bands at 2090 and 2025 $cm^{-1}$ are at lower frequency than expected for a cationic rhodium (III) dicarbonyl complex (cf. $\nu$(CO) 2118, 2087 $cm^{-1}$ for [Cp*Rh(CO)$_2$Me]$^+$, unpublished results; 2144, 2101 $cm^{-1}$ for [Tp*Ir(CO)$_2$H]$^+$, ref 14).
(23) As the 2090 and 2025 $cm^{-1}$ bands decay, there is some gain in IR absorbance in the region of the 2057 $cm^{-1}$ peak of the reactant **1e** and the 2069 $cm^{-1}$ peak of the acetyl product **3e**. There is also an apparent shift to higher frequency of the 1982 $cm^{-1}$ band of **1e** toward the end of the experiment, leaving a long-lived absorption at 1987 $cm^{-1}$, suggesting the formation of some additional unidentified species.

first-order rate constants reported in the Supporting Information and plotted in Figure 4 are lower (by a factor of ca. 2) than those obtained in the absence of Proton Sponge, consistent with a competing reaction being quenched. The rate constant and activation parameters derived from these data are given in Table 3.

**Reactivity of [Bp*Rh(CO)(L)] (L = $PPh_3$, 6d; L = CO, 6e).** In view of the change in Tp* coordination mode which accompanies the reaction of **1a**−**d** with MeI, it was of interest to compare their reactivity with that of analogous bis(pyrazolyl)borate (Bp*) complexes which lack the pendant pyrazolyl group. The dicarbonyl **6e** was made by the method of Trofimenko,[24] and subsequent substitution of a CO ligand in **6e** by $PPh_3$ gave the phosphine complex **6d**.[25] The similarity of $\nu$(CO) for the two square planar $PPh_3$ complexes (**1d**, 1978 $cm^{-1}$; **6d**, 1980 $cm^{-1}$) reflects their similar coordination environments. However, **1d** and **6d** show markedly different reactivity toward methyl iodide. Whereas the Tp* complex **1d** reacted readily to give a cationic methyl product **2d**, the Bp* complex **6d** reacted much more slowly and with more complicated kinetic behavior. The decay of the $\nu$(CO) band of **6d** was accompanied by the appearance of an absorption at 1690 $cm^{-1}$ assigned to an acetyl ligand, with only a very weak feature at 2065 $cm^{-1}$ in the region expected for a Rh(III) methyl species. Although no pure product was isolated from this reaction, the spectroscopic data suggest slow oxidative addition to give a methyl intermediate, [Bp*Rh(CO)($PPh_3$)(Me)I], followed by rapid methyl migration to give [Bp*Rh($PPh_3$)(COMe)I] **7d**. A kinetic plot of the 1980 $cm^{-1}$ band of **6d** (298 K, 2.0 M MeI in $CH_2Cl_2$) showed that it did not follow a simple exponential decay, despite the pseudo-first-order conditions employed. The decay was slow and approximately linear for the initial 2 h, but then the rate increased such that all of the reactant complex was consumed after ca. 5 h. Under identical conditions **1d** reacted with MeI with a half-life of ca. 10 min. A rough quantitative comparison of relative reactivity was obtained from the initial rates, which showed **1d** to be more reactive by a factor of ca. 20. Thus the presence of the third pyrazolyl group is key in determining the reactivity in these systems.

Further reactivity tests were performed using the dicarbonyl, **6e**. In this case the coordination geometry differs from the Tp* version **1e**, in which the Tp* ligand adopts $\kappa^3$ coordination. The lower electron density on Rh induced by the loss of a coordinated pyrazolyl group is reflected by the shift in $\nu$(CO) to higher frequency for **6e** (2081, 2013 $cm^{-1}$) relative to **1e** (2057, 1981 $cm^{-1}$). The reaction of **6e** with MeI led to formation of a product with $\nu$(CO) at 2075 and 1724 $cm^{-1}$, assigned to terminal and acetyl CO ligands in [Bp*Rh(CO)(COMe)I] **7e**. There was no evidence for detectable amounts of any intermediate methyl complex. A kinetic plot of the 2013 $cm^{-1}$ band of **6e** (308 K, 8.0 M MeI, $CH_2Cl_2$) again deviated from exponential behavior and displayed a sigmoid curve, with all the reactant complex being consumed in ca. 3 h. Extrapolation of the rate data obtained for **1e** predicts a half-life of ca. 1 min under identical conditions, again illustrating the difference in reactivity between Bp* and Tp* complexes. The reactivity of **6d** and **6e** toward $CH_3I$ is summarized in Scheme 6.

**Scheme 6.** Reactions of **6d** (L = $PPh_3$) and **6e** (L = CO) with MeI

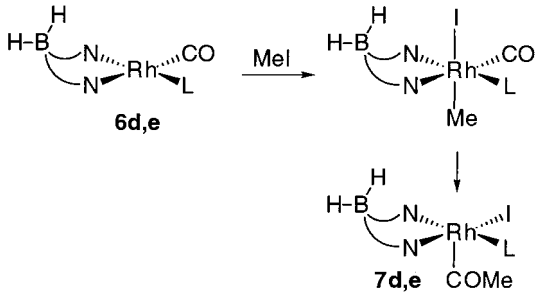


**Reaction Mechanism.** The results reported above highlight the key role of the third pyrazolyl group in the reactivity of [Tp*Rh(CO)(L)], whether it is coordinated in the ground state of the reactant (L = CO) or not (L = phosphine). Scheme 7 illustrates three alternative routes by which the reaction of [Tp*Rh(CO)(L)] with MeI might occur. In route i, there is an initial preequilibrium between $\kappa^2$ and $\kappa^3$ isomers, with the $\kappa^3$ species acting as nucleophile toward MeI. It is expected that the higher electron density bestowed on Rh by coordination of the third pyrazolyl group will render it more nucleophilic. In the case of L = CO, the $\kappa^3$ isomer already predominates and direct nucleophilic attack by the 18-electron metal center can occur (as is the case for the isoelectronic Cp*Rh$(CO)_2$[15,26]). Structural studies have shown that the complexes **1a**−**d** with L = phosphine exist as the $\kappa^2$ isomers, both in the solid state and in solution.[8−11] Inspection of the X-ray crystal structures for **1a**, **c**, and **d** shows that a simple rotation of the pendant pyrazolyl group (by ca. 90−100°) about its N−B bond is all that is required to achieve $\kappa^3$ coordination with square pyramidal geometry at Rh. The transient existence of the $\kappa^3$ form has been proposed to explain the exchange of pyrazolyl groups observed for complexes **1a**−**d** by $^1$H NMR spectroscopy.[8,9,11] The pyrazolyl group trans to phosphine was found to exchange more rapidly with uncoordinated pyrazolyl than that trans to CO, indicative of a square pyramidal transition state or intermediate. The subtle balance between $\kappa^2$ and $\kappa^3$ coordination modes is also illustrated by the one-electron oxidation of **1d** to give **1d**$^+$ in which the third pyrazolyl group binds to Rh in a square pyramidal structure.[10,11] Thus, lower electron density on the metal center favors a $\kappa^2 \rightarrow \kappa^3$ isomerization. Route ii in Scheme 7 differs from route i only in that coordination of the third pyrazolyl group is concerted with nucleophilic attack by Rh on MeI, rather than stepwise. In route iii the $\kappa^2 \rightarrow \kappa^3$ isomerization occurs only after the formation of the Rh−Me bond. In this scenario, the pendant pyrazolyl arm serves to trap a five-coordinate 16-electron cation, leaving the iodide released in the process as counterion.

(24) Trofimenko, S. *J. Am. Chem. Soc.* **1967**, *89*, 6288.
(25) Bonati, F.; Minghetti, G.; Banditelli, G. *J. Organomet. Chem.* **1975**, *87*, 365.
(26) Bassetti, M.; Monti, D.; Haynes, A.; Pearson, J. M.; Stanbridge, I. A.; Maitlis, P. M. *Gazz. Chim. Ital.* **1992**, *122*, 391.

**Scheme 7.** Alternative Mechanistic Pathways for Reaction of **1a**−**d** with MeI

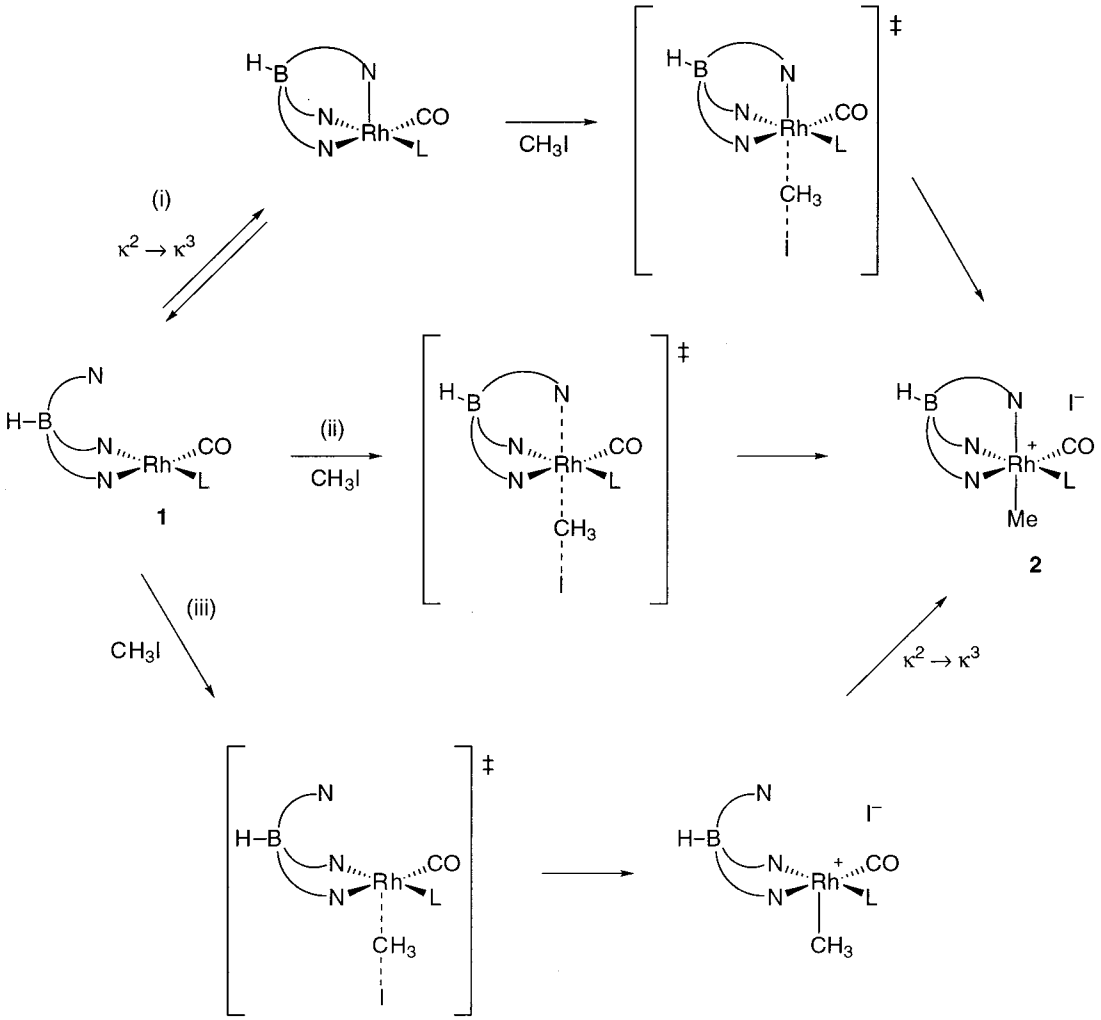


For each of the three routes shown in Scheme 7, rate-determining nucleophilic attack by Rh on MeI would lead to the observed second-order kinetics and large negative entropies of activation. However, route iii would only give the observed lower reactivity for the Bp* analogues if the $S_N2$ process were reversible. On this basis, and because of the known facility for changes in ligand denticity in the reactant complexes and related Rh species,[27] we favor routes i and ii in which complete or partial Rh−N bond formation has occurred at the transition state for the $S_N2$ process. It is known that a potentially coordinating neighboring group can assist oxidative addition in other systems. For example, reaction of the Vaska-type complex, *trans*-[Ir(CO){$PMe_2$-Ar}$_2$Cl], with MeI is ca. 100× faster when Ar is 2-$MeOC_6H_4$ than when Ar is 4-$MeOC_6H_4$ or $C_6H_5$, indicating that the $S_N2$ transition state is stabilized by an interaction of the iridium center with an *o*-methoxy substituent.[28] In that case, however, the Ir−O interaction is only transient, and coordination of iodide gives [Ir(CO)($PMe_2Ar$)$_2$ClIMe] as the product.

The switch from $\kappa^2$ to $\kappa^3$ coordination of the Tp* ligand accompanying oxidative addition resembles some recent observations on the mechanism of C−H activation by Tp* complexes. For example, in the photochemically induced activation of alkanes by **1e**,[29] the C−H oxidative addition step is thought to occur while the Tp* ligand is $\kappa^2$ coordinated, but subsequent rechelation generates the stable Rh(III) alkyl hydride with a $\kappa^3$ Tp* ligand.[30] The necessity for these two bonding modes is shown by the failure of the Bp* complex **6e** to activate alkanes,[20] just as we find that the absence of a third pyrazolyl group markedly lowers the reactivity toward MeI. Similar pathways have been proposed for reductive elimination of methane from [$\kappa^3$-Tp*Rh($CNCH_2$-$CMe_3$)(Me)H][31] and oxidative addition of alkanes to [$\kappa^2$-Tp*PtMe] (generated by methyl anion abstraction from [$\kappa^2$-

(27) Malbosc, F.; Kalck, P.; Daran, J.-C.; Etienne, M. *J. Chem. Soc., Dalton Trans.* **1999**, 271. Paneque, M.; Sirol, S.; Trujillo, M.; Gutiérrez-Puebla, E.; Monge, M. A.; Carmona, E. *Angew. Chem., Int. Ed.* **2000**, *39*, 218. Paneque, M.; Sirol, S.; Trujillo, M.; Carmona, E.; Gutierrez-Puebla, E.; Monge, M. A.; Ruiz, C.; Malbosc, F.; Le Berre, C. S.; Kalck, P.; Etienne, M.; Daran, J.-C. *Chem. Eur. J.* **2001**, *7*, 3868. Bucher, U. E.; Currao, A.; Nesper, R.; Rueegger, H.; Venanzi, L. M.; Younger, E. *Inorg. Chem.* **1995**, *34*, 66.

(28) Miller, E. M.; Shaw, B. L. *J. Chem. Soc., Dalton Trans.* **1974**, 480.

(29) Ghosh, C. K.; Graham, W. A. G. *J. Am. Chem. Soc.* **1987**, *109*, 4726. Bloyce, P. E.; Mascetti, J.; Rest, A. J. *J. Organomet. Chem.* **1993**, *444*, 223.

(30) Bromberg, S. E.; Yang, H.; Asplund, M. C.; Lian, T.; McNamara, B. K.; Kotz, K. T.; Yeston, J. S.; Wilkens, M.; Frei, H.; Bergman, R. G.; Harris, C. B. *Science* **1997**, *278*, 260.

(31) Wick, D. D.; Reynolds, K. A.; Jones, W. D. *J. Am. Chem. Soc.* **1999**, *121*, 3974.

$Tp^*PtMe_2]^-$).[32] It has also been shown that protonation or methylation of Pt(II) complexes $[\kappa^2\text{-}Tp'PtR_2]^-$ (Tp′ = Tp, Tp*) leads to $[\kappa^3\text{-}Tp^*PtR_2(H/Me)]$.[33]

**Effect of Phosphine Ligand.** It is clear from the kinetic data in Table 3 that the reactivity of phosphine complexes **1a**−**d** toward MeI increases with the phosphine basicity, i.e., $k_2$ increases in the order $PPh_3 < PMePh_2 < PMe_2Ph < PMe_3$. At the extremes of this series, the $PMe_3$ complex **1a** has a rate constant ca. 45 times larger than the $PPh_3$ complex **1d**, corresponding to a lowering of $\Delta G^{\ddagger}_{298}$ by ca. 9 kJ mol$^{-1}$. Comparison of the activation parameters for the reactions of **1a** and **1d** suggests that the difference in reactivity can be ascribed mainly to a lowering of $\Delta H^{\ddagger}$. The activation parameters for **1b** also fit this trend, but those for **1c** are somewhat anomalous, suggesting an larger entropic contribution to the difference in reactivity of **1a** and **1c**. The lack of a smooth trend in activation parameters for the series **1a**−**d** may reflect the possibility that the measured rate constant $k_2$ is actually a composite of the equilibrium constant for $\kappa^2 \rightarrow \kappa^3$ isomerization and the rate constant for nucleophilic attack by the $\kappa^3$ species, as depicted in route i of Scheme 7. Also, both steric and electronic factors will contribute to the overall activation barrier, which may lead to the observed irregularity in the trend for $\Delta H^{\ddagger}$.

Similar trends in reactivity toward MeI have been found for other series of complexes, e.g., [CpCo(CO)(L)][34] and [Cp′Ir(CO)(L)] (Cp′ = Cp or Cp*).[35] Angelici et al. demonstrated the existence of a linear free energy relationship between log $k_2$ and the basicity of the coordinated phosphine, as measured by its enthalpy of protonation ($-\Delta H_{HP}$) by triflic acid in 1,2-dichloroethane.[36] Linearity was observed provided very sterically hindered phosphines (e.g., $PCy_3$) were not included in the fit. Figure 5 shows a plot of log $k_2$ vs $-\Delta H_{HP}$ for our series of Tp* complexes **1a**−**d** together with plots of the data reported for [CpCo(CO)(L)] and [Cp′Ir(CO)(L)]. A linear dependence on phosphine basicity is found for the reactions of **1a**−**d**, obeying the equation log $k_2 = (-6.9 \pm 0.6) + (0.17 \pm 0.02)(-\Delta H_{HP})$ ($R = 0.981$). The slope of this plot is similar to those for [Cp*Ir(CO)(L)] ($0.16 \pm 0.02$) and [CpIr(CO)(L)] ($0.14 \pm 0.01$) reported by Wang and Angelici.[37] The very similar dependence of nucleophilicity on phosphine basicity displayed by tris(pyrazolyl)borate and cyclopentadienyl complexes shows that their reaction mechanisms are closely related. The consistently lower reactivity of the Tp* complexes in our study (i.e., more negative intercept in Figure 5) is probably due to the greater steric bulk of the Tp* ligand[38] (cone angle 224° when $\kappa^3$ coordinated compared to 142° for Cp*) although a more direct comparison using the same metal would require rate data for the [Cp*Rh(CO)(L)] series.

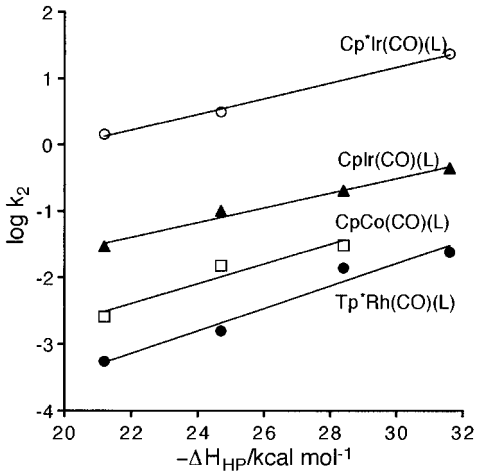


**Figure 5.** Plot of log $k_2$ vs phosphine ligand basicity (measured by $-\Delta H_{HP}$) for reactions of **1a**−**d** with MeI. Corresponding plots are also shown for cyclopentadienyl Co and Ir complexes.[35]

The reaction rates for **1a**−**d** were also compared with other parameters which measure phosphine basicity. The linearity of a plot of log $k_2$ against the Derencsényi parameter ($\delta$ $^{31}$P of $R_3P{=}O$)[39] was rather poor ($R = 0.83$), but a better linear correlation ($R = 0.983$) was found using Tolman's electronic parameter ($\nu(CO)(A_1)$ of $[Ni(CO)_3(L)]$).[40] Surprisingly, a poor correlation ($R = 0.92$) was found when log $k_2$ was plotted against $\nu$(CO) (measured in $CH_2Cl_2$) for complexes **1a**−**d** themselves. This is mainly because $\nu$(CO) for **1d** occurs 1 cm$^{-1}$ *lower* in frequency than that for **1c**, despite the fact that $PPh_3$ is a poorer donor than $PPh_2Me$.[41] A possible explanation for this apparent discrepancy is provided by the X-ray crystal structures[8−11] of **1a**, **1c**, and **1d**, which (despite each showing square planar geometry with $\kappa^2$ Tp* coordination) reveal a shorter Rh···N distance to the third pyrazolyl group in **1d** (3.537(5) Å) than in **1c** (3.661(4) Å) or **1a** (3.632(3) Å). It appears from the IR data that this shift from $\kappa^2$ toward $\kappa^3$ coordination imparts higher electron density than expected on the Rh center of **1d**.

The relative electron-donating ability of Tp and Cp ligands has been a matter of some debate (as recently summarized by Tellers et al.[42]) and appears to vary as a function of the metal, its oxidation state, and the other ligands in the complex. The $\nu$(CO) bands of $[Tp^*Rh(CO)_2]$ **1e** (2057, 1981 cm$^{-1}$ in $CH_2Cl_2$) are significantly higher in frequency than those of $[Cp^*Rh(CO)_2]$ (2018, 1950 cm$^{-1}$), suggesting that Cp* is the better donor for these group 9 M(I) complexes. Despite this, the two dicarbonyl complexes have very similar nucleophilicity toward MeI ($10^4$ $k_{obs}/s^{-1} = 5.4$ for **1e** and 4.6 for $[Cp^*Rh(CO)_2]$[26] at 298 K, 0.8 M MeI in $CH_2Cl_2$).

(32) Wick, D. D.; Goldberg, K. I. *J. Am. Chem. Soc.* **1997**, *119*, 10235.
(33) Reinartz, S.; Brookhart, M.; Templeton, J. L. *Organometallics* **2002**, *21*, 247. Canty, A. J.; Dedieu, A.; Jin, H.; Milet, A.; Richmond, M. K. *Organometallics* **1996**, *15*, 2845. O'Reilly, S. A.; White, P. S.; Templeton, J. L. *J. Am. Chem. Soc.* **1996**, *118*, 5684.
(34) Hart-Davies, A. J.; Graham, W. A. G. *Inorg. Chem.* **1970**, *9*, 2658.
(35) Wang, D.; Angelici, R. J. *Inorg. Chem.* **1996**, *35*, 1321.
(36) Sowa, J. R. J.; Zanotti, V.; Facchin, G.; Angelici *J. Am. Chem. Soc.* **1991**, *113*, 9185.
(37) The fit parameters quoted from ref 35 for $[Cp'Ir(CO)(PR_3)]$ include data for additional phosphine ligands not included in the plots shown in Figure 5.
(38) Han, R.; Parkin, G. *Organometallics* **1991**, *10*, 1010.
(39) Derencsényi, T. T. *Inorg. Chem.* **1981**, *20*, 665.
(40) Tolman, C. A. *Chem. Rev.* **1977**, *77*, 313.
(41) The $\nu$(CO) observed for **1d** in the solid state (1965 cm$^{-1}$, KBr disk) shows an even larger anomaly compared with the values for **1a**, **1b**, and **1c** (1961, 1968, 1975 cm$^{-1}$, respectively). We also note that $\nu$(BH) for this series of complexes follows the unusual order **1a** < **1d** < **1b** < **1c** (data from ref 9).
(42) Tellers, D. M.; Skoog, S. J.; Bergman, R. G.; Gunnoe, T. B.; Harman, W. D. *Organometallics* **2000**, *19*, 2428.

This similarity is difficult to account for, since both steric and electronic factors predict that **1e** should be less nucleophilic than [Cp*Rh(CO)$_2$]. One possible explanation for the higher than expected reactivity of **1e** is the driving force provided by the high propensity of the Tp* ligand to achieve a 6-coordinate environment, especially in low-spin d$^6$ systems. Complex **1e** is also similar in reactivity to the $PPh_3$ complex **1d** (Table 3), indicating that the better donor ability of $PPh_3$ compared with CO is offset by its steric bulk.

The nucleophilicity of **1a**−**d** can also be compared with rate data for other square planar Rh(I) complexes. The second-order rate constants reported in Table 3 are all at least an order of magnitude higher than that for the carbonylation catalyst, [Rh(CO)$_2$I$_2$]$^-$ ($2.9 \times 10^{-5}$ M$^{-1}$ s$^{-1}$, 25 °C),[43] reflecting the increased electron density on Rh imparted by the P and N donor ligands. Interestingly, the $PMe_3$ complex **1a** reacts with MeI ca. 18 times faster than the Vaska analogue, *trans*-[Rh(CO)(PEt$_3$)$_2$I],[16,44] despite the $\nu$(CO) frequency of **1a** being higher by 8 cm$^{-1}$.[45] Similarly, the $PPh_3$ complex, **1d**, reacts ca. 16 times faster than *trans*-[Rh(CO)(PPh$_3$)$_2$Cl].[46,47] Clearly steric as well as electronic factors are important in determining metal nucleophilicity.[17]

## Conclusions

Reaction of square planar Rh(I) complexes [$\kappa^2$-Tp*Rh(CO)(L)] **1a**−**d** with MeI gives products of the form [$\kappa^3$-Tp*Rh(CO)(L)Me]$^+$I$^-$ **2a**−**d** (L = phosphine). Coordination of the third pyrazolyl group in the pseudooctahedral Rh(III) product effectively traps the cationic intermediate resulting from nucleophilic attack by Rh(I) on MeI. The iodide anion displaced in this reaction remains as counterion, rather than coordinating to Rh to complete the formal oxidative addition process. These results further strengthen the evidence in favor of a two-step $S_N2$ mechanism for oxidative addition of MeI to square planar d$^8$ transition metal complexes. Kinetic measurements indicate second-order behavior, with large negative activation entropies, consistent with a highly ordered $S_N2$ transition state. Since $\kappa^2 \rightarrow \kappa^3$ isomerism in the reactant complexes **1a**−**d** is indicated by fluxional exchange of the pyrazolyl groups, it is proposed that the third Rh−N bond is at least partially formed at the transition state for the reaction with MeI (i.e., routes i or ii in Scheme 7). The second-order rate constants correlate well with phosphine basicity (as measured by the protonation enthalpy of $PR_3$ or the Tolman electronic parameter), and with the relative reaction rates reported for related series of complexes [Cp′M(CO)(L)] (Cp′ = Cp, Cp*; M = Co, Ir). The bis(pyrazolyl)borate complexes [$\kappa^2$-Bp*Rh(CO)(L)] (L = $PPh_3$, CO) **6d**,**e** are much less reactive toward MeI than the Tp* analogues, indicating the importance of the third pyrazolyl group. The methyl complexes **2a**−**d** isomerize slowly in solution to give neutral acetyl species [$\kappa^3$-Tp*Rh(L)(COMe)I]. By contrast, no methyl intermediate is observed in the reaction of the dicarbonyl **1e** with MeI, which leads directly to an acetyl complex [$\kappa^3$-Tp*Rh(CO)(COMe)I] **3e**.

## Experimental Section

**General.** All manipulations were performed under nitrogen using standard Schlenk techniques. Solvents were distilled under nitrogen, toluene from sodium/benzophenone and dichloromethane from $CaH_2$. Commercial phosphines were used without further purification. Complexes **1a**−**e** were prepared as previously described,[8,9] and Bp* complexes **6e**[24] and **6d**[25] were synthesized according to literature procedures. NMR spectra were recorded on a Bruker AMX 400 spectrometer. Routine infrared spectra were recorded on a Perkin-Elmer 1710 or a Mattson Genesis FTIR spectrometer, the latter being used to monitor kinetic experiments (vide infra).

**Synthesis of Rhodium Complexes. (a) [Tp*Rh(CO)(PMe$_3$)(Me)]I 2a.** Methyl iodide (13.6 $\mu$L, 0.22 mmol) was added in the dark to a toluene solution of [Tp*Rh(CO)(PMe$_3$)] **1a** prepared in situ as described previously[9] from the reaction of **1e** (100 mg, 0.22 mmol) and a stoichiometric amount of $PMe_3$. After 4 h of agitation, a white precipitate was observed. Agitation was maintained overnight, and the white precipitate was then filtered under an inert atmosphere and was dried under vacuum. Recrystallization at −18 °C from dichloromethane/heptane afforded translucent crystals; yield 94 mg (60%). A suitable crystal was selected for an X-ray diffraction study (vide infra). IR ($CH_2Cl_2$): $\nu$(CO)/cm$^{-1}$ 2080. NMR (400 MHz, $CD_2Cl_2$, 233 K, *J* in Hz): $\delta$ $^1$H 1.59 (br, 3 H, dd at 293 K; $^2J_{Rh-H}$ 3.1, $^3J_{P-H}$ 1.8, Rh−C*H*$_3$), 1.86 (b, 9 H, $^2J_{P-H}$ 11.4, P(C*H*$_3$)$_3$), 2.25, 2.28, 2.35, 2.37, 2.38, 2.40 (all s, 18 H, *H*$_3$C−pz*), 5.85 (br, 1 H, *H*C-pz*), 5.96, 5.98 (both s, 2 H, *H*C-pz*), 4.5 (br, B−*H*); $\delta$ $^{31}$P {$^1$H} 10.52 (d, $^1J_{Rh-P}$ 98.2); $\delta$ $^{13}$C {$^1$H} −1.72 (dd, $^1J_{Rh-C}$ 17.4, $^2J_{P-C}$ 6.3, Rh−*C*H$_3$), 12.36, 12.38, 12.92, 13.81, 15.81, 16.08 (all s, H$_3$*C*−pz*), 16.67 (d, $^1J_{P-C}$ 36.7, P(*C*H$_3$)$_3$), 107.14 (d, $J_{P-C}$ 3.6, H*C*-pz*), 107.68, 109.65 (all s, H*C*-pz*), 144.9 (d, $J_{P-C}$ 3.0, H$_3$C*C*−pz*), 145.97 (s, H$_3$C*C*−pz*), 146.18 (s, H$_3$C*C*−pz*), 149.87 (d, $J_{P-C}$ 2.7, H$_3$C*C*−pz*), 150.35 (s, H$_3$C*C*−pz*), 151.68 (s, H$_3$C*C*−pz*), 184.0 (dd, $^1J_{Rh-C}$ 61.3, $^2J_{P-C}$ 17.7, *C*O); $\delta$ $^{103}$Rh 1111.

**(b) [Tp*Rh(CO)(PMe$_2$Ph)(Me)]I 2b.** Methyl iodide (27.3 $\mu$L, 0.44 mmol) was added in the dark to a dichloromethane solution of [Tp*Rh(CO)(PMe$_2$Ph)] **1b** prepared in situ as described previously[9] from the reaction of **1e** (200 mg, 0.44 mmol) and a stoichiometric amount of $PMe_2Ph$. The reaction solution was stirred for 4 h, after which recrystallization at −18 °C from dichloromethane/heptane afforded white crystals. IR ($CH_2Cl_2$): $\nu$(CO)/cm$^{-1}$ 2082. NMR (400 MHz, $CD_2Cl_2$, 233 K, J in Hz): $\delta$ $^1$H 1.95 (d, $^2J_{P-H}$ 11.06, PC*H*$_3$), 2.07 (d, $J_{P-H}$ 8.1, PC*H*$_3$) 1.65 (Rh−C*H*$_3$), 1.91, 2.06, 2.23, 2.26, 2.29, 2.38, 2.41, (all s, *H*$_3$C−pz*), 5.76, 5.85, 5.93 (all s, *H*C-pz*), 7.4 (m, P*Ph*), 4.5 (B−*H*); $\delta$ $^{31}$P {$^1$H} 14.03 (d, $^1J_{Rh-P}$ 100.2); $\delta$ $^{13}$C {1H} −0.34 (dd, $^1J_{Rh-P}$ 17.3; $^2J_{P-C}$ 6.18; Rh−*C*H$_3$), 12.38, 12.49, 12.81, 13.8, 15.32, 15.47 (all s, H$_3$*C*−pz*), 15.80 (d, $^1J_{P-C}$ 36.9, P(*C*H$_3$)), 17.13 (d, $^1J_{P-C}$ 36.3, P*C*H$_3$), 107.16 (d, $J_{P-C}$ 3.2; H*C*-pz*), 107.76, 109.45 (all s, H*C*-pz*), 128.69 (d, $J_{P-C}$ 10.9, P*Ph*), 129.56 (d, $J_{P-C}$ 55.33, P*Ph*), 129.32 (d, $J_{P-C}$

(43) Haynes, A.; Mann, B. E.; Morris, G. E.; Maitlis, P. M. *J. Am. Chem. Soc.* **1993**, *115*, 4093.
(44) Rankin, J.; Poole, A. D.; Benyei, A. C.; Cole-Hamilton, D. J. *Chem. Commun.* **1997**, 1835.
(45) We note that comparison of $\nu$(CO) values between different series of complexes may mislead regarding the relative electron densities on the metal center. The lower $\nu$(CO) value for *trans*-[Rh(CO)(PEt$_3$)$_2$Cl] (1961 cm$^{-1}$) compared with **1a** (1969 cm$^{-1}$) can be ascribed to the position of the CO ligand trans to a $\pi$-donor ligand (Cl) in the former complex rather than to greater net electron density on Rh. For the same reason $\nu$(CO) for [Rh(CO)(dppe)I] (CO trans to P) is markedly higher than for *trans*-[Rh(CO)(PPh$_3$)$_2$I] (CO trans to I) (ref 46).
(46) Douek, I. C.; Wilkinson, G. *J. Chem. Soc. A* **1969**, 2604.
(47) The value ($5.5 \times 10^{-4}$ s$^{-1}$) given for [Rh(CO)(PPh$_3$)$_2$Cl] in ref 46 is a pseudo-first-order rate constant, which we have divided by the concentration of neat MeI (16 M) to estimate the second-order rate constant for comparison with **1d**.

9.3, P*Ph*), 131.38 (s, P*Ph*), 145.01 (d, $J_{P-C}$ 3.01, $H_3$CC-pz*, 146.19, 146.24 (each s, $H_3$CC-pz*), 149.86 (d, $J_{P-C}$ 3.13, $H_3$CC-pz*), 150.90, 152.32 (each s, $H_3$C*C*-pz*), 184.02 (dd, $^1J_{Rh-C}$ 60.9, $^2J_{P-C}$ 16.9, *C*O); $\delta$ $^{103}$Rh 1169.

**(c) [Tp*Rh(PMe$_3$)(COMe)I] 3a.** Complex **2a** (10.5 mg, 0.008 mmol) was dissolved in $CD_2Cl_2$, and NMR spectroscopy indicated complete conversion to complex **3a** after several days. The red product was recrystallized by slow evaporation of the $CD_2Cl_2$ from the NMR tube, and a suitable crystal was selected for an X-ray diffraction study (vide infra). IR (KBr): $\nu$(CO)/cm$^{-1}$ 1670. NMR (400 MHz, $CD_2Cl_2$, 233 K, J in Hz): $\delta$ $^1$H 1.54 (d, $^2J_{P-H}$ 10.7, P(C*H*$_3$)$_3$), 2.09 (s, C(O)C*H*$_3$), 2.13, 2.37, 2.40, 2.43, 2.44, 2.54 (all s, *H*$_3$C−pz*), 5.78, 5.86, 5.92 (all s, *H*C-pz*), 4.6 (b, B−*H*); $\delta$ $^{31}$P {$^1$H} 2.1 (d, $^1J_{Rh-P}$ 130.8); $\delta$ $^{13}$C {$^1$H} 12.45, 12.85, 13.20, 16.60, 16.71, 19.65 (all s, $H_3$*C*-pz*), 18.83, (d, $^1J_{P-C}$ 34.8, P(*C*H$_3$)$_3$), 106.92 (d, $J_{P-C}$ 34.41, H*C*-pz*), 107.19, 107.78 (all s, H*C*-pz*), 143.70 (s, $H_3$C*C*-pz*), 144.25 (d, $J_{P-C}$ 2.5, $H_3$C*C*-pz*), 145.32 (s, $H_3$C*C*-pz*), 150.02 (s, $H_3$C*C*-pz*), 151.53 (s, $H_3$C*C*-pz*), 151.63 (d, $J_{P-C}$ 3.8, $H_3$C*C*-pz*), 230.7 (dd, $^1J_{Rh-C}$ 23.8, $^2J_{P-C}$ 8.2, *C*(O)CH$_3$); $\delta$ $^{103}$Rh 2945.

**(d) [Tp*Rh(COMe)(CO)I] 3e.** A solution of methyl iodide and dichloromethane (10 cm$^3$; 1:4 v/v) was added to **1e** (50 mg, 0.11 mmol). The reaction mixture was stirred at room temperature for 2.5 h, after which time the IR spectrum showed bands at 2068 and 1682 cm$^{-1}$, consistent with [Tp*Rh(COMe)(CO)I] **3e**. Reduction of the solvent to a minimum and cooling to 0 °C afforded the product as a dark red solid, which was isolated by filtration. $^1$H NMR spectroscopy and elemental analysis indicated the presence of unidentified impurities, probably byproducts resulting from N-protonation of the Tp* ligand (vide supra). Yield: 51 mg (77%). Anal. Calcd for ($C_{18}H_{25}RhBIN_6O_2$): C, 36.14; H, 4.22; N, 14.05; I, 21.22. Found C, 34.54; H, 4.23; N, 13.47; I, 19.64. IR ($CH_2Cl_2$): $\nu$(CO)/cm$^{-1}$ 2068 and 1679. NMR ($CDCl_3$): $\delta$ $^1$H 5.77, 5.80, 5.85 (all s, 3 H, *H*C-pz*), 2.65 (3 H, s, COC*H*$_3$), 2.30−2.40 (all s, 18 H, *H*$_3$C-pz*).

**(e) [$\kappa^2$-HB(3,5-Me$_2$pz)$_2$(3,5-Me$_2$pzH)Rh(CO)(PPh$_3$)]BF$_4$ 4d.** Complex **1d** (40 mg, 0.058 mmol) was dissolved in $CH_2Cl_2$ (7 cm$^3$), and to the resulting solution was added $HBF_4$·$Et_2O$ (9 $\mu$L, 1 equiv). After 5 min the IR spectrum showed a shift of $\nu$(CO) from 1978 to 1988 cm$^{-1}$. The solvent was removed and the residue recrystallized from $CH_2Cl_2$/$Et_2O$, giving an orange solid. Yield: 34 mg (76%). Anal. Calcd for ($C_{34}H_{38}RhB_2F_4N_6OP$): C, 52.47; H, 4.93; N, 10.80. Found: C, 52.09; H, 5.11; N, 9.55. IR ($CH_2Cl_2$): $\nu$(CO)/cm$^{-1}$ 1988. NMR ($CDCl_3$): $\delta$ $^1$H 12.05 (1H, s, N−*H*), 7.50 (15 H, m, PPh$_3$), 5.90, 5.68, 5.55 (all s, 3 H, *H*C-pz*), 2.40, 2.25, 1.76, 1.70, 1.35 (all s, 18 H, *H*$_3$C−pz*); $\delta$ $^{31}$P 41.90 (d, $J_{Rh-P}$ 158).

**(f) [$\kappa^2$-HB(3,5-Me$_2$pz)$_2$(3,5-Me$_2$pzH)Rh(CO)(Me)(I)(PPh$_3$)]BF$_4$ 5d.** To a solution of **4d** in $CH_2Cl_2$, prepared as described above, was added methyl iodide (1.25 cm$^3$, excess). The reaction was monitored for 1 week using IR spectroscopy. During this time, the reaction mixture changed color from orange to red and a new absorption began to appear at 2094 cm$^{-1}$, assigned to [$\kappa^2$-HB(3,5-Me$_2$pz)$_2$(3,5-Me$_2$pzH)Rh(CO)(Me)(I)PPh$_3$]BF$_4$ **5d**. Isolation and further characterization of the product was not attempted.

**X-ray Crystal Structure Determinations for 2a and 3a.** For both compounds, the data were collected at room temperature (293 K) on a Stoe imaging plate diffraction system (IPDS). The crystal-to-detector distance was 80 mm; 250 exposures (3 min/exposure) were obtained with $0° < \varphi < 250°$ and with the crystals oscillated through 1° for **2a** and 29° for **3a** in $\varphi$. Coverage of the unique set was over 91% complete to at least 24.3°. Crystal decay was monitored by measuring 200 reflections per image. Final unit cell parameters were obtained by the least-squares refinement of 2000 reflections. Only statistical fluctuations were observed in the intensity monitors over the course of the data collection.

**Table 4.** Crystallographic Data for **2a** and **3a**

| crystal params | **2a**·$CH_2Cl_2$ | **3a** |
|---|---|---|
| compound | [$BC_{20}H_{34}N_6OPRh$]I·$CH_2Cl_2$ | $BC_{20}H_{34}IN_6OPRh$ |
| fw (g) | 731.06 | 646.13 |
| shape (color) | box (colorless) | box (orange) |
| size, mm | 0.43, 0.35, 0.13 | O.52, 0.24, 0.20 |
| cryst syst, space group | triclinic, *P*1 | triclinic, *P*1 |
| *a*, Å | 10.237(2) | 11.556(3) |
| *b*, Å | 12.395(2) | 14.144(3) |
| *c*, Å | 13.238(3) | 15.684(3) |
| $\alpha$, deg | 77.45(2) | 93.18(2) |
| $\beta$, deg | 67.77(2) | 97.25(2) |
| $\gamma$, deg | 80.40(2) | 93.92(2) |
| *V*, Å$^3$ | 1511.1(5) | 2531(1) |
| *Z* | 2 | 4 |
| *F*(000) | 715 | 1280 |
| $\rho$(calcd), g/cm$^{-3}$ | 1.605 | 1.693 |
| $\mu$ (Mo K$\alpha$), cm$^{-1}$ | 18.200 | 19.536 |
| | Data Collection | |
| diffractometer | IPDS Stoe | IPDS Stoe |
| radiation | Mo K$\alpha$ ($\lambda$ = 0.71073) | Mo K$\alpha$ ($\lambda$ = 0.71073) |
| scan mode | $\Phi$ | $\Phi$ |
| detector dist, mm | 80 | 80 |
| $\phi$ range, deg | $0 < \phi < 250$ | $0 < \phi < 250$ |
| $\phi$ incr, deg | 1.0 | 2.0 |
| exposure time, min | 3 | 3 |
| 2$\theta$ range, deg | $6.4 < 2\theta < 47.8$ | $3.6 < 2\theta < 48.5$ |
| abs correction | numerical (X-shape) | numerical (X-shape) |
| min/max transm | 0.470/0.828 | 0.513/0.738 |
| no. of reflns collected | 11373 | 19955 |
| no. of unique reflns ($R_{int}$) | 4237 (0.026) | 7466 (0.052) |
| reflns used | 3337 ($I > 2\sigma(I)$) | 5671 ($I > 3\sigma(I)$) |
| | Refinement | |
| *R* | 0.0294 | 0.0640 |
| $R_w$ | 0.0348 | 0.0633 |
| weighting scheme | Chebyshev | Chebyshev |
| coeff $A_r$ | 2.10, −0.843, 1.60 | 2.83, −0.485, 2.25, −0.15 |
| GOF | 1.077 | 1.068 |
| $(\Delta/\sigma)_{max}$ | 0.033 | 0.029 |
| $\Delta\rho_{min}/\Delta\rho_{max}$ | −0.58/0.68 | −3.2/2.2 |
| ls params | 312 | 568 |

The structures were solved by direct methods (SIR92)[48] and refined by least-squares procedures on $F_{obs}$. H atoms were located on difference Fourier maps, but those attached to C atoms were introduced in calculation in idealized positions ($d$(CH) = 0.96 Å) and their atomic coordinates were recalculated after each cycle. They were given isotropic thermal parameters 20% higher than those of the carbon to which they are attached. The coordinates and the isotropic temperature factors of the H atoms attached to the B atoms were refined. Least-squares refinements were carried out by minimizing the function $\sum w(|F_o| - |F_c|)^2$, where $F_o$ and $F_c$ are the observed and calculated structure factors. The weighting scheme used in the last refinement cycles was $w = w'[1 - (\Delta F/6\sigma(F_o)^2]^2$ where $w' = 1/\sum_1^n A_r T_r(x)$ with three coefficients $A_r$ for the Chebyshev polynomial $A_r T_r(x)$ where $x$ was $F_c/F_c$(max).[49] Models reached convergence with $R = \sum(||F_o| - |F_c||)/\sum(|F_o|)$ and $R_w$ =

(48) Altomare, A.; Cascarano, G.; Giacovazzo, G.; Guagliardi, A.; Burla, M. C.; Polidori, G.; Camalli, M. SIR92—a program for automatic solution of crystal structures by direct methods. *J. Appl. Crystallogr.* **1994**, *27*, 435.

(49) Prince, E. *Mathematical Techniques in Crystallography*; Springer-Verlag: Berlin, 1982.

$[\sum w(|F_o| - |F_c|)^2/\sum w(F_o)^2]^{1/2}$, having values listed in Table 4. Criteria for a satisfactory complete analysis were the ratios of rms shift to standard deviation less than 0.1 and no significant features in final difference maps. Details of data collection and refinement are given in Table 4. The calculations were carried out with the CRYSTALS package programs[50] running on a PC. The drawings of the molecules were realized with the help of CAMERON.[51]

**Kinetic Experiments.** Samples for kinetic runs were prepared by placing the required amount of freshly distilled methyl iodide (and Proton Sponge when appropriate) in a 2 $cm^3$ graduated flask, which was then made up to the mark with the solvent of choice (usually $CH_2Cl_2$). A small portion of this solution was used to record a background spectrum. Another portion (1 $cm^3$) was added to the solid metal complex (ca. 8 $\mu$mol) in a sample vial to initiate the reaction. A sample of the reaction solution was quickly transferred to the IR cell, and the kinetic experiment was started. In order to obtain pseudo-first-order conditions, at least a 10-fold excess of MeI was used, relative to the metal complex. The IR cell (0.5 mm path length, $CaF_2$ windows) was maintained at constant temperature throughout the kinetic run by a thermostated jacket. Spectra were scanned in the metal carbonyl $\nu$(CO) region (2200−1600 $cm^{-1}$) and saved at regular time intervals under computer control. After the kinetic run, absorbance vs time data for the appropriate $\nu$(CO) frequencies were extracted and analyzed off-line using Kaleidagraph curve-fitting software. The decays of the bands due to **1a**−**e** were all well fitted by exponential curves with correlation coefficients $\geq$0.999, to give pseudo-first-order rate constants. Each kinetic run was repeated at least twice, the $k_{obs}$ values given being averaged values with component measurements deviating from each other by $\leq$5%.

**Acknowledgment.** The Groupe Electrochimie de la Direction des Etudes et Recherches of Electricité de France (fellowship to V.C.) and the EPSRC (studentship to C.E.H.) are thanked for financial support of this study. We thank Dr. Nigel Wheatley for helpful discussions.

**Supporting Information Available:** Tables of kinetic data (PDF). X-ray crystallographic data for **2a** and **3a** (CIF). This material is available free of charge via the Internet at http://pubs.acs.org.

IC0255959

(50) Watkin, D. J.; Prout, C. K.; Carruthers, J. R.; Betteridge, P. W. *CRYSTALS Issue 10*; Chemical Crystallography Laboratory: Oxford, U.K., 1996.

(51) Watkin, D. J.; Prout, C. K.; Pearce, L. J. *CAMERON*; Chemical Crystallography Laboratory: Oxford, U.K., 1996.